

Co-Firing Oil Shale with Coal and Other Fuels for Improved Efficiency and Multi-Pollutant Control

33rd International Technical Conference on Coal Utilization & Fuels Systems

Richard D. Boardman
Robert A. Carrington
William C. Hecker
Reed Clayson

June 2008

The INL is a
U.S. Department of Energy
National Laboratory
operated by
Battelle Energy Alliance



This is a preprint of a paper intended for publication in a journal or proceedings. Since changes may be made before publication, this preprint should not be cited or reproduced without permission of the author. This document was prepared as an account of work sponsored by an agency of the United States Government. Neither the United States Government nor any agency thereof, or any of their employees, makes any warranty, expressed or implied, or assumes any legal liability or responsibility for any third party's use, or the results of such use, of any information, apparatus, product or process disclosed in this report, or represents that its use by such third party would not infringe privately owned rights. The views expressed in this paper are not necessarily those of the United States Government or the sponsoring agency.

Co-Firing Oil Shale with Coal and Other Fuels for Improved Efficiency and Multi-Pollutant Control

**Richard D. Boardman, Robert A. Carrington - Idaho National Laboratory
William C. Hecker- Brigham Young University, Reed Clayson Synthetic Energy Development**

Abstract

Oil shale is an abundant, undeveloped natural resource which has natural sorbent properties, and its ash has natural cementitious properties. Oil shale may be blended with coal, biomass, municipal wastes, waste tires, or other waste feedstock materials to provide the joint benefit of adding energy content while adsorbing and removing sulfur, halides, and volatile metal pollutants, and while also reducing nitrogen oxide pollutants.

Oil shale depolymerization-pyrolysis-devolatilization and sorption scoping studies indicate oil shale mineral particle sorption rates and sorption capacity can be comparable to limestone sorbents for capture of SO₂ and SO₃. Additionally, kerogen released from the shale was shown to have the potential to reduce NO_x emissions through the well established "reburning" chemistry similar to natural gas, fuel oil, and micronized coal. Productive mercury adsorption is also possible by the oil shale particles as a result of residual fixed-carbon and other observed mercury capture sorbent properties. Sorption properties were found to be a function particle heating rate, peak particle temperature, residence time, and gas-phase stoichiometry. High surface area sorbents with high calcium reactivity and with some adsorbent fixed/activated carbon can be produced in the corresponding reaction zones that exist in a standard pulverized-coal or in a fluidized-bed combustor.

Background

Previous research has demonstrated that ground oil shale addition to a fluidized-bed combustor can enhance power generation by; 1) serving as a natural, highly effective acid-gas absorbent for both coal and municipal solids waste (MSW), 2) creating a cementitious ash that materially reduces the potential for leaching "hazardous" materials from the ash, and possibly serving as a viable building material, 3) adding heating value to the fuel input, and, in the case of MSW, significantly improving combustion options for power generation, and 4) relieving the strain on available landfills and perhaps lessening the risk of leaching from existing and new landfills.¹

Oil shale is found in several prehistoric marine deposits in the United States and throughout the world. It is characterized by banded carbonate and oxide minerals laden with a polymer organic residue called kerogen. In order to discriminate oil shale "richness" or grade, the relative amount of oil in gallons per ton (gpt) of a given oil shale rock is determined using an approximate procedure called the Modified Fischer Assay. Some recovery techniques may produce slightly more than the amount indicated by the Fischer Assay; however, it provides a useful measurement to compare one deposit with another. A fairly contiguous zone of 25 gpt or more extends through the Green River Formation in Colorado, Utah, and Wyoming. In Colorado and Utah, where it is known as the Mahogany Zone, it averages about 100 feet in thickness. Roughly 85% of the Mahogany shale is mineral matter with a typical composition reported listed in Table 1. Some U.S. oil shale also contains Dolomite (CaMg(CO₃)₂), Nahcolite (NaHCO₃), and Dawsonite (NaAl(OH)₂CO₃) which are relatively abundant in many samples. Similar quality oil shale is found in Russia, China, Israel, India, Australia, Morocco, Venezuela, and other minor countries. Israeli shale, however, contains upwards of 75% CaCO₃.

¹ Clayson and McCarthy: Niche Market Assessment for a Small-Scale Western Oil Shale Project, DOE Contract DE-FC21-86MC11076, July, 1989.

The approximate heating value of the 25 gpt Mahogany oil shale is roughly 2,200 Btu/lb (HHV) and therefore is not suitable for direct combustion or gasification in any standard gasifier. Even 50-60 gpt oil shale is difficult to ignite and maintain self-heating and combustion in either a fixed-bed or fluid-bed reactor.

Table 1. Average Mineral Composition of Mahogany Zone Shale²

Mineral	Chemical Form	Composition (wt%)
<i>Ankerite</i>	$\text{Ca}(\text{Mg}_{1-x}, \text{Fe}_x)(\text{CO}_3)_2$	32
<i>Calcite</i>	CaCO_3	16
<i>Quartz</i>	SiO_2	15
<i>Illite</i>	$\text{KAl}_2(\text{AlSi}_3)\text{O}_{10}(\text{OH})_2$	19
<i>Albite</i>	$\text{NaAlSi}_3\text{O}_8$	10
<i>K Feldspar</i>	KAlSi_3O_8	6
<i>Pyrite</i>	FeS_2	1
<i>Analcime</i>	$\text{NaAlSiO}_4 \cdot 25\text{H}_2\text{O}$	1
	Total	100

The reaction kinetics of oil shale depolymerization/pyrolysis/devolatilization (DPD) and decomposition of carbonate minerals is covered in various principal references.^{2,3,4,5,6} Most of these studies were carried out at slow to only moderate heating rates (0.5-50 K/min) that are attainable in laboratory thermogravimetric analysis (TGA) instruments and typically only for large particles. Only the reference by Wen provides data on the heating rates, peak temperatures, and time scales reminiscent of a pulverized-coal boiler (i.e., 10,000 K/sec) for pulverized particles (45-75 μm diameter). Consequently, while the results of these studies may be relevant to dual-fired oil shale applications in either a fluidized-bed or fixed-bed application, they do not apply to small particles subjected to rapid heating rates (on the order of 10^4 - 10^5 °C/min) injected into an entrained-flow pulverized coal combustor or gasifier.

Purpose & Scope

The purpose of the present study was to obtain a better understanding of oil shale particle devolatilization and sorption kinetics in order to develop new oil shale applications, including the possible injection of ground oil shale into a pulverized-coal boiler to adsorb SO_2 and SO_3 . The potential for adsorption of heavy metals released during coal combustion, especially mercury and arsenic, was also postulated. It was further recognized that the kerogen in the oil shale particles could be exploited in the same manner that coal, oil, and natural gas are currently used to manipulate flame stoichiometry in order to reduce nitrogen oxide pollutants to benign nitrogen. The technical feasibility of using oil shale as a multi-pollutant control agent was investigated by:

- Selecting, obtaining, grinding, and classifying oil shale samples meeting prescriptive composition and physical specifications from three separate oil-shale deposits in Colorado and obtaining a representative limestone (dolomite) sample for comparative sorption testing
- Completing thermodynamic predictions to determine theoretical oil shale sorbent capacities at optimum reaction conditions and to gain insight regarding the selectivity of oil shale for H_2S adsorption over CO_2 , for example

² J.H. Campbell, The Kinetics of Decomposition of Colorado Oil Shale: II: Carbonate Minerals, Lawrence Livermore Laboratory, UCRL-52089 Part 2, March, 1978

³ O. Bekri, H.Baba-Habib, Y.C. Chang, and M.C. Edelman, "Study of Oil Shale Thermal Decomposition Kinetics," Sixteenth Oil Shale Symposium Proceedings, Colorado School of Mines Press, 1983; M.F. Singleton, et. al, 1982

⁴ A. K. Burnham, "Reaction Kinetics and Diagnostics for Oil Shale Retorting, Lawrence Livermore Laboratory, UCRL-86794, October, 1981

⁵ R.J. Cena and R. G. Mallon, "Results and Interpretation of Rapid-Pyrolysis Experiments Using the LLNL Solid-Recycle Oil Shale Retort," in Nineteenth Oil Shale Symposium Proceedings, Colorado School of Mines Press, p 102, August, 1986

⁶ R.J. Cena and R. G. Mallon, "Results and Interpretation of Rapid-Pyrolysis Experiments Using the LLNL Solid-Recycle Oil Shale Retort," in Nineteenth Oil Shale Symposium Proceedings, Colorado School of Mines Press, p 102, August, 1986

- Completing flat-flame and drop-tube furnace tests to investigate small particle shale depolymerization/dpolymerization/devolatilization and calcination kinetics and behavior at various heating rates and gas compositions
- Thermally conditioning some particles by injection into the aft flame zone of a down-fired gas research combustor in order to achieve the high heating rates and time-temperature conditions representative of a full-scale pulverized combustor
- Completing shale sorbent reactions scoping studies for SO₂, H₂S, and mercury with the thermally conditioned particles, and
- Completing chemical kinetic mechanism studies to determine the potential NO_x reduction efficiency of shale volatile hydrocarbons and char-containing particles.

Oil Shale Sample Preparation and Characterization

Three unique samples of Green River Shale were selected for the present work. Raw oil shale from the COLORADOA site oil shale mine, set aside by the U.S. DOE in the 1970's for oil shale research and production demonstrations, were obtained from the government steward of the C-A site. Figure 1 shows the shale rubble in its "as received" condition, consisting of shale ranging from 1 to 5-inch coarse irregular rocks. Dark bands of oil shale are evident in this exhibit, which illustrates that the oil shale is not homogeneous in any sense. Two additional grades of Green River oil shale with oil an oil content of 45 gpt and 15 gpt were obtained from outcroppings around the Grand Junction, Colorado area.



Figure 1. Green River Oil Shale Rubble Collected from the C-A mine site in the Piceance Creek area near Meeker, Colorado.

The raw shale was crushed, ground and sieved to three sizes fractions; 75-90 μm (200-170 Tyler Mesh), 125-210 μm (110-65 Tyler Mesh), and 500-1000 μm (34-17 Tyler Mesh). The smallest particle diameter is the upper size particle preferable for air entrainment and injection through a pulverized coal-fired boiler burner. Due to the oily residues in the 45 gpt shale, 75-90 μm was the smallest unconsolidated practical size that could be practically achieved while avoiding excessive heat, clumping, and premature devolatilization of the kerogen in the particles. This size fraction also corresponds to earlier sulfur capture studies for injected limestone particles.⁷ The largest size fraction was obtained to compare results to classical limestone particle sulfur adsorption studies⁸ that were selected

⁷ Borgwardt, R. H., 1970. "Kinetics of the Reaction of SO₂ with Calcined Limestone," *Env. Sci. and Technol.* **4**, 59-63

⁸ Fenouil, L. A., and Lynn S., 1995. "Study of Calcium-Based Sorbents for High Temperature H₂S Removal." 1. Kinetics of H₂S Sorption by Uncalcined Limestone, 2. Kinetics of H₂S Sorption by Calcined Limestone, and 3. Kinetics of H₂S Sorption by Calcined Limestone. *Ind. Eng. Chem. Res.* **34**, 2324-2348.

to benchmark the current work. The ground and classified samples were packed with a nitrogen gas blanket in 500-gram containers.

Table 2. Oil Shale Sample Proximate, Ultimate, Mineral Matter, and Toxic Metals Analyses

Parameter	B Units	15 gpt Shale B Result	30 gpt Shale A Result	45 gpt Shale B Result	A Units
Moisture	Wt %	0.3	0.05	0.5	Wt%, ar
Volatile Matter	Wt %	19.17	41.03	38.24	Wt%, ar
Fixed Carbon	Wt %	<0.1	<0.1	<0.1	Wt%, ar
Ash	Wt %	80.71	59.84	62.9	Wt%, ar
Carbon ^a	Wt %	6.82	24.48	23.49	Wt%, ar
Oxygen	Wt %	11.6	11.4	9.2	Wt%, ar
Hydrogen	Wt %	0.42	2.28	2.52	Wt%, ar
Nitrogen	Wt %	0.25	0.86	1.17	Wt%, ar
Sulfur, total	Wt %	0.2	1.14	0.74	Wt%, ar
Ash	Wt %	80.71	59.84	62.9	Wt%, ar
TOTAL Ultimate Analysis		100	100	100	
Silica (SiO ₂)	Wt %	56.79	44.42	49.49	Wt%, dry
Calcium Oxide (CaO)	Wt %	14.31	22.77	18.25	Wt%, dry
Aluminum Oxide (Al ₂ O ₃)	Wt %	10.33	10.33	10.05	Wt%, dry
Magnesium Oxide (MgO)	Wt %	6.76	6.40	7.96	Wt%, dry
Ferric Oxide (Fe ₂ O ₃)	Wt %	3.76	4.02	4.61	Wt%, dry
Potassium Oxide (K ₂ O)	Wt %	3.28	2.20	3.04	Wt%, dry
Sodium Oxide (Na ₂ O)	Wt %	2.77	4.60	2.66	Wt%, dry
Sulfur Trioxide (SO ₃)	Wt %	0.86	3.88	2.45	Wt%, dry
Phosphate Pentoxide (P ₂ O ₅)	Wt %	0.19	0.65	0.48	Wt%, dry
Titanium Oxide (TiO ₂)	Wt %	0.46	0.53	0.42	Wt%, dry
Barium Oxide (BaO)	Wt %	0.14	<0.01	0.14	Wt%, dry
Manganese Oxide (MnO)	Wt %	0.1	0.03	0.11	Wt%, dry
Strontium Oxide (SrO)	Wt %	0.08	0.17	0.1	Wt%, dry
Chlorine, Total	Wt %	0.0013	0.05	0.0052	Wt%, ar
Total Mineral Matter		99.8	100.1	99.8	
Copper	µg/g	13	<5	48	mg/kg, dry
Chromium	µg/g	65	75	39	mg/kg, dry
Nickel	µg/g	29	<5	27	mg/kg, dry
Cobalt	µg/g	12	-	8	mg/kg, dry
Arsenic	µg/g	<4	217	<4	mg/kg, dry
Lead	µg/g	<20	<5	<20	mg/kg, dry
Mercury	µg/g	<0.1	0.3	<0.1	mg/kg, dry
Heating Value			4001 (HHV)		BTU/lb, ar
Calculated gpt			43		

a. Wt. % carbon include inorganic carbonates that are released during test analysis

Table 2 presents the oil shale composition in terms of 1) proximate analysis (i.e., weight percent moisture, volatile matter, fixed carbon, and ash), 2) ultimate analysis (i.e., weight percent carbon, oxygen, hydrogen, nitrogen, total sulfur, and ash), 3) mineral matter in the ash (reported as oxides of base specific metalloids in the ash, and 4) trace metals- specifically toxic metals such as mercury, arsenic, lead, chromium, and nickel. The analytical results reveal that the shale collected and believed to be 30 gpt has a measured heating rate consistent with 45 gpt shale. Therefore, it should be recognized that 30 gpt samples test results referenced in this report are in fact higher.

Thermodynamic and Mass Transfer Considerations

Figure 2 shows a plot of the thermodynamic stability and dissociation of calcium compounds containing sulfate, phosphate, oxide, and hydrate (lime) phases. Below 750°C SO₂ is predicted to be adsorbed by the mineral phase. Above 750°C, some sulfate compounds begin to dissociate, however, CaSO₄ does not decompose to CaO until the solid temperature reaches approximately 1200°C. Above 1300°C, the calcium is predicted to be completely calcined, with the exception of some Ca₃(PO₄)₂ which does not dissociate until high temperatures are observed. Hence, 1200°C represents the maximum temperature where calcium will adsorb SO₂ under the prediction conditions. The behavior of magnesium compounds (Figure 3) is similar to calcium, except that the predictions indicate MgSO₄ dissociates above 750°C. Figures 4 shows similar sulfate compound formation and dissociation thermodynamics for sodium. The same behavior was exhibited by potassium, although K₂SO₄ begins to decompose around 1000°C. Alkaline metals with chloride and phosphate theoretically become volatile above 1200°C in a similar manner to alkaline sulfates. While these calculations indicate the possible concurrent reactivity of alkali species with halide gases, such as HCl and H₂PO₄, they also reveal potential volatility of the alkaline compounds. Such behavior is similar to the alkaline compounds commonly found in coal fly ash.

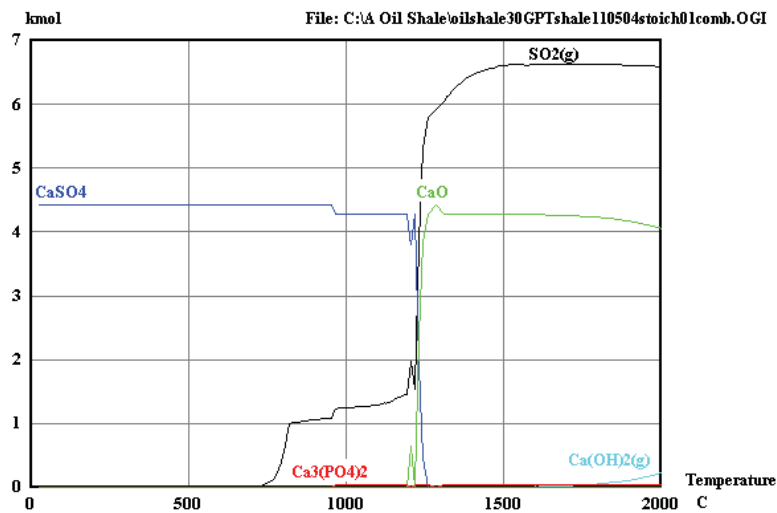


Figure 2. Ca-Sulfate-Phosphate compound dissociation trends.

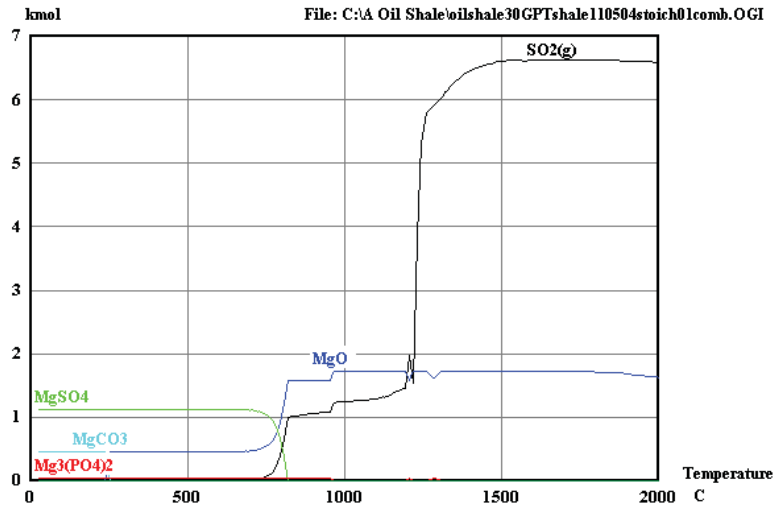


Figure 3. Mg-Sulfate-Phosphate compound dissociation trends.

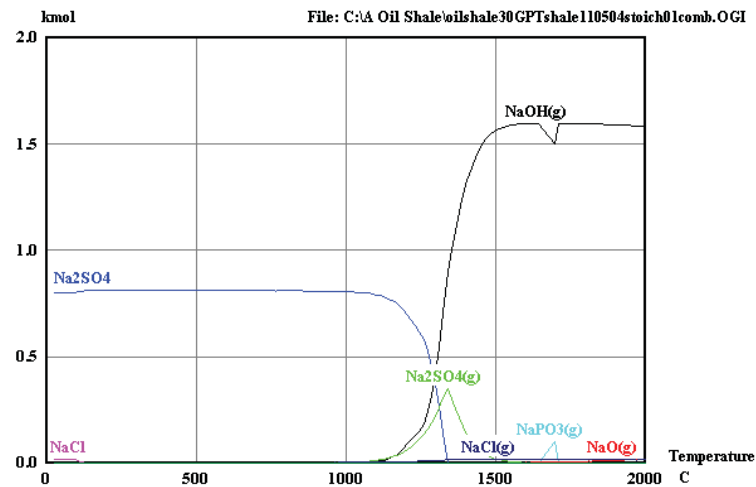


Figure 4. Na-Sulfate-Chloride compound dissociation trends.

Bulk gas diffusion, pore diffusion in the solids, and solid state diffusion through the CaSO_4 product layer preclude stoichiometric reaction of all sulfur with the available calcium. Since the molar volume of CaSO_4 is higher than CaCO_3 , the process steps of (1) dissociating CaCO_3 , (2) adsorbing SO_2 and SO_3 and (3) forming CaSO_4 can result in pore closure before all of the reactive Ca sites in a particle are utilized. This phenomenon limits the practical conversion of Ca and Mg in limestone and dolomite sorbent particles to around 15-20%.⁹ In the case of the oil shale sorbent particles, however, it is anticipated that the pore structure and pore volume resulting from devolatilization of the kerogen will provide greater access to the available reactive mineral species. Hence, although oil shale has less weight percent calcium and magnesium, it was postulated that up to 100% reaction with sulfur pollutants could be possible.

⁹ R.D. Boardman, B.S. Brewster, Z. Haque, L.D. Smoot, and G.D. Silcox, "Modeling Sorbent Injection and Sulfur Capture in Pulverized Coal Combustion, Transactions of the ASME, FACT-Vol. 15, Air Toxic Reduction and Combustion Modeling, 1992.

Depolymerization/Pyrolysis/Devolatilization Scoping Tests

In addition to standard thermo-gravimetric (TGA) mass loss measurements at a heat-up rate of 20 K/min, a drop-tube furnace (DTF), an updraft flat-flame burner (FFB), and a down-fired multi-fuels entrained-particle reactor (MFR, illustrated in Figure 5) was used to investigate small particle DPD behavior.¹⁰

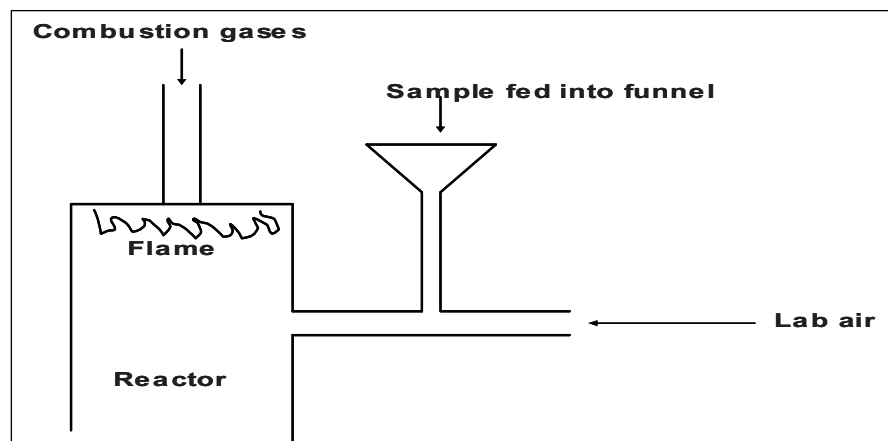


Figure 5. Combustor setup used to thermally condition entrained oil shale particles

Figure 6a shows a group of typical TGA ramp curves (wt% vs. time) at 7 K/min. Figure 6b shows the corresponding plots of dm/dt . The first mode occurs when the organic kerogen is depolymerized and then devolatilized. The second mode principally corresponds to carbonate dissociation. Figure 7 shows BET surface area increasing with the heating rate. High surface area and high porosity are both key to obtaining high sorption rates and capacities. Figure 8 compares the hydrogen to carbon ratio of the raw shale versus particles subjected to the differing heating rates of the flat flame burner, multi-fuel reactor, and drop-tube furnace.

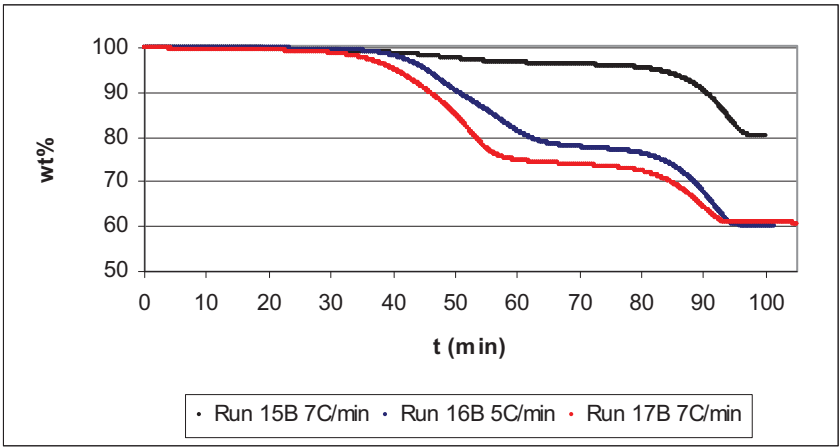
A summary of the measured mass release and resulting surface areas as a function of heating rate, oil shale grade, and particle size for the separate experimental reactors is presented in Table 3. These results indicate that DPD mass loss and particle surface are a strong function of particle heating rate and can be cross correlated with oil shale grade and particle size. Optimum surface areas and particle properties for acid pollutant sorbents are achieved at high heating rates (i.e., high temperature reactor conditions); however, fixed-carbon retention is favored at slow heating rates with moderate-size particles. These results help understand possible benefits and trade-offs for practical applications. For example, high surface particles laden with fixed carbon are considered optimum for mercury adsorption.

The reaction availability of CaO was determined by measuring the calcium surface area using TGA to measure CO₂ uptake for calcined particle samples. At 300 °C CaO adsorbs CO₂ to form CaCO₃. The CaO surface area can then be calculated using the equation below. The measured CaO surface areas listed in Table 5. The limited data preclude discernment of any trend; however, it can be seen in general that the CaO surface area is higher than the nitrogen adsorption BET surface area. Sample 12 exhibits a relatively low dispersion and CaO reactivity and may be an outlier, possibly due to the heterogeneous nature of the samples.

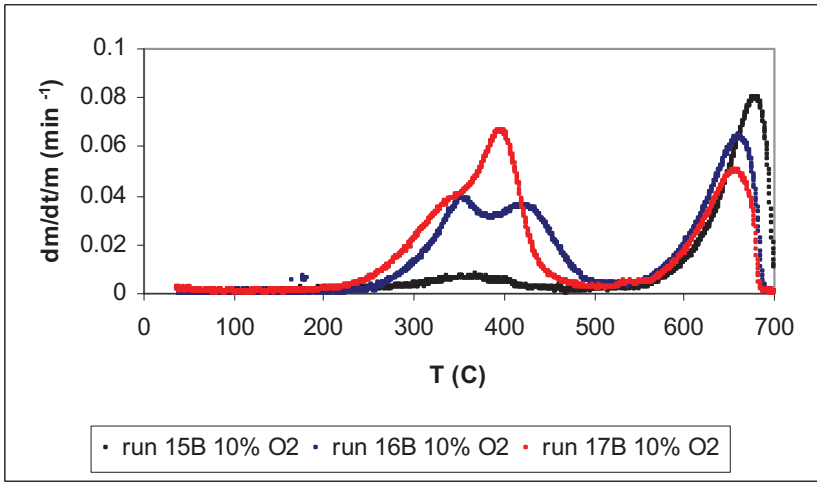
$$SA_{CaO} = \frac{1573 \cdot (Wt \%_{129 \text{ min}} - Wt \%_{91 \text{ min}})}{Wt \%_{9 \text{ min}}}$$

- Weight percents can be found from TGA test results.

¹⁰ DPD tests were performed by Brigham Young University Chemical Engineering faculty and students using test reaction setups of the Advanced Combustion Engineering Research Center, Test Report to INL, August, 2004.



(a)



(b)

Figure 6. (a) A typical ramp test curve as displayed on the TGA. (b). the corresponding dw/dt curves. sample 15 (black), sample 16 (blue), sample 17 (red).

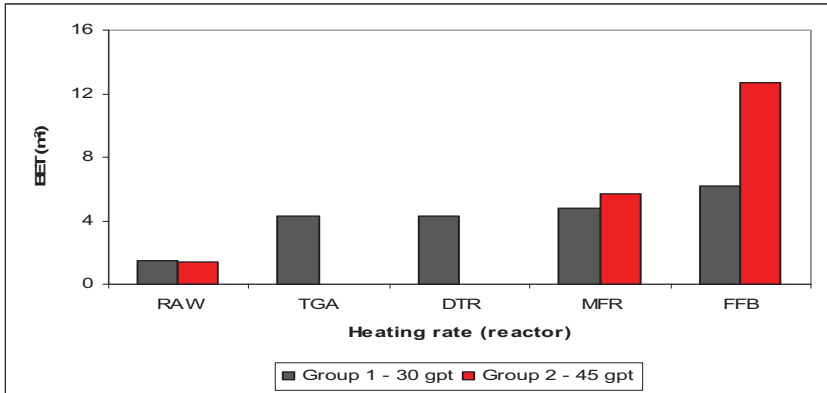


Figure 7. The effect of heating rate on BET surface area per gram

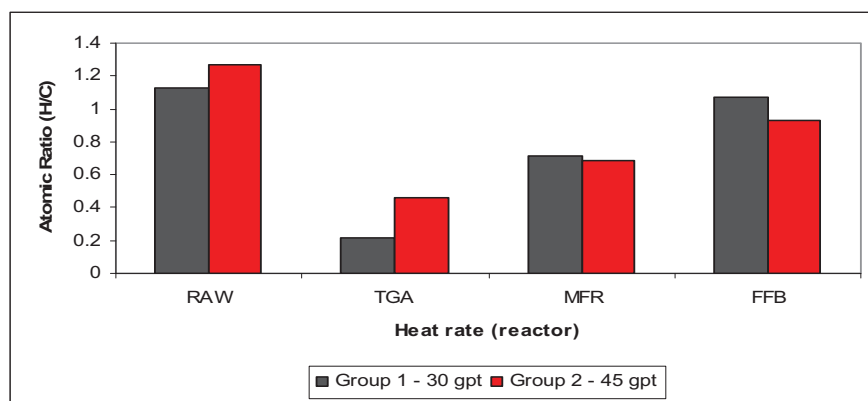


Figure 8. The effect of heating rate on Atomic H/C.

Table 4 Particle Surface Area Results as a Function of Particle Grade, Heating Rate, and D_p

Sple No.	Reactor Grade D_p	Heating Rate (K/min)	Mass release %	BET area m^2/gm	Stdev. m^2/gm	Sple No.	Reactor Grade D_p	Heating Rate (K/min)	Mass release %	BET area m^2/gm	Stdev. m^2/gm
1	FFB 15 gpt 90 μm	100,000	71	4.2	0.228	11	MFR 15 gpt 90 μm	10,000	67	4.9	0.165
2	FFB 30 gpt 90 μm	100,000	60	6.2	0.277	12	MFR 30 gpt 90 μm	10,000	87	4.8	0.380
3	FFB 45 gpt 90 μm	100,000	65	12.7	0.516	13	MFR 45 gpt 90 μm	10,000	68	5.8	0.581
4	FFB 30 gpt 200 μm	100,000	32	1.6	0.152	14	MFR 30 gpt ~700 μm	10,000	72	2.5	0.132
5	DTR 30 gpt 90 μm	40,000	45	4.2	0.354	15	Raw 15 gpt 90 μm	N/A	0	1.9	0.028
6	DTR 30 gpt 200 μm	40,000	81	8.5	0.100	16	Raw 30 gpt 90 μm	N/A	0	1.5	0.025
7	TGA 15 gpt 90 μm	20 K/min	34	4.6	0.244	17	Raw 45 gpt 90 μm	N/A	0	1.4	0.061
8	TGA 30 gpt 90 μm	20 K/min	70	4.3	0.032	18	Raw 30 gpt 200	N/A	0	0.4	0.053
9	TGA 30 gpt 200 μm	20 K/min	68	2.7	0.213	19	Raw 30 gpt ~700 μm	N/A	0	0.1	0.023
10	TGA 45 gpt 90 μm	20 K/min	76	15.8	0.316						

FFB -Flat Flame Burner; DTR – Drop Tube Reactor; TGA – Thermogravimetric Ramp Reactor; MFR – (Gas/Entrained-Particle) Multifuel Fuel Reactor; Raw – Untreated oil shale particles; gpt – gallon per ton of kerogen in shale; D_p – particle diameter in micro-meters

Table 5: Calcium Oxide surface areas

Sample Number	1	2	3	4	8	11	12	13
Oil Shale Grade	15	30	45	30	30	15	30	45
Devolatilization Reactor	FFB	FFB	FFB	FFB	TGA	MFR	MFR	MFR
CaO Surface Area (m^2/gm)	12.6	15.6	10.2	15.8	20.9	14.4	4.9	26.8
Percent Dispersion (%)	5.1	6.3	4.6	6.4	9.3	-	2.0	-

Sulfur and Mercury Sorption Scoping Tests

A differential reactor similar in design to previous calcination and sulfur sorbent tests was used to conduct particle sorption capacity tests.¹¹ Figure 9 compares calcium SO₂ sorption reactivity versus oil shale grade, sorbent particle size, and differential reactor tube temperature. Nearly quantitative conversion of CaO to CaSO₄ in 30 and 45 gpt grade shale is achieved at 870°C, while particle sintering, pore closure, and solid-phase diffusion were jointly determined to inhibit sorbent reactivity at higher temperatures. The reactivity also appears to be cross correlated with sorbent particle area and weight, as postulated. Figure 10 compares the SO₂ sorption capacity of 30 gpt oil shale sorbent with a reference dolomite limestone. Closely comparable sorption is achieved with the oil shale in spite of containing significantly less weight percent calcium and magnesium. This suggests the pore volume and available practical CaO reaction capacity is approximately equal for the samples tested.

NO_x Reactivity Potential

FTIR results of the DPD tests indicate that the organic functional groups and light hydrocarbons evolved during rapid pyrolysis of small oil shale particles are serendipitously tailored for NO_x reduction. This is converse to waxy oils that are evolved at low heating rates, such as those encountered in oil shale retorting devices. NO_x levels in the gas/entrained-particle multi-fuel reactor were shown to be reduced at high loadings of raw oil-shale and fuel-rich gas stoichiometry. The Chemkin™ kinetics management code was used to demonstrate that 70-85% reduction of NO_x (based on an input of 1000 ppm NO_x exiting the flame zone) can be achieved by staging a fuel-rich zone produced exclusively by oil shale volatiles with tertiary air input into the upper boiler and super-heater sections of a pulverized-coal combustor. This result is plotted in Figure 11.

Practical Applications

Figures 12 illustrate a possible application for using oil shale to reduce pollutant emissions in a pulverized-coal combustor. The INL has licensed this application to Nalco Mobotec. Pilot-plant tests are being conducted Nalco Mobotec to determine the potential for NO_x reduction and pollutant sorption in at residence times and reactor conditions typical of a pulverized-coal boiler.

Alternatively, it may be desirable to produce the oil shale via ex-situ gasification or combustion of the oil shale. This deployment may allow optimization of multi-pollutant control by injecting the reducing gas produced by retorting the shale into the coal boiler at the optimum location, while allowing for injection of the calcined shale into the combustor at the optimum gas and temperature for SO₂/SO₃ adsorption and for optimum mercury adsorption.

Acknowledgments

This laboratory study and concept development was completed under a three-year project with funding through the INL Laboratory-Directed Research and Development Program. Experimental testing was completed with the support of university student interns Angela Kohler (BYU), Jason Pickup (Utah State), and Rhett Finch (BYU), along with the support of INL laboratory technicians Ron Leanna and Cal Johnson. Combustion Resources, Provo Utah, obtained, characterized and provided the ground oil shale under a subcontract to the project. The Brigham Young University Catalysis Laboratory was subcontracted to conduct the particle devolatilization and calcination studies completed under the present effort.

¹¹ Fenouil L. A., and Lynn S., 1995. "Study of Calcium-Based Sorbents for High Temperature H₂S Removal." 1. Kinetics of H₂S Sorption by Uncalcined Limestone, 2. Kinetics of H₂S Sorption by Calcined Limestone, and 3. Kinetics of H₂S Sorption by Calcined Limestone. *Ind. Eng. Chem. Res.* **34**, 2324-2348.

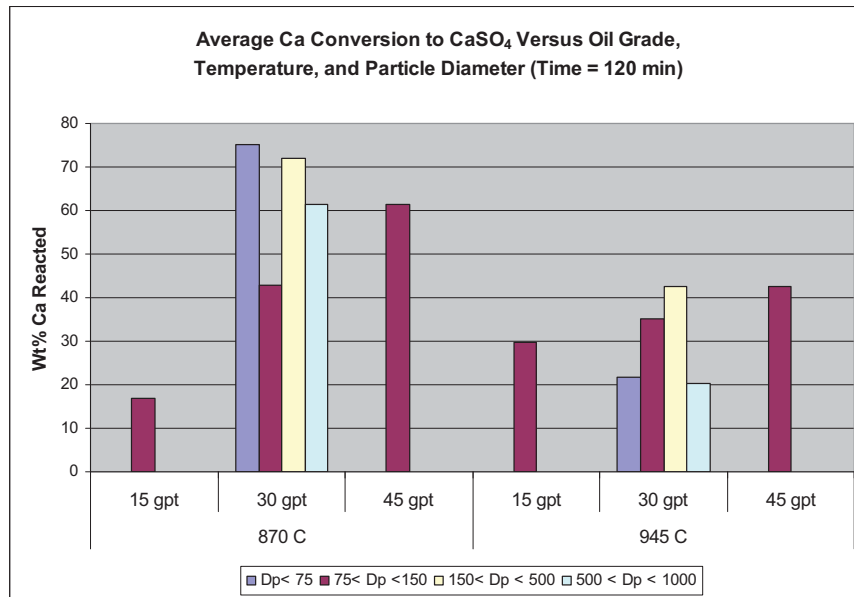


Figure 9. Comparison of calcium reactivity as a function of oil shale grade, temperature, and particle size.

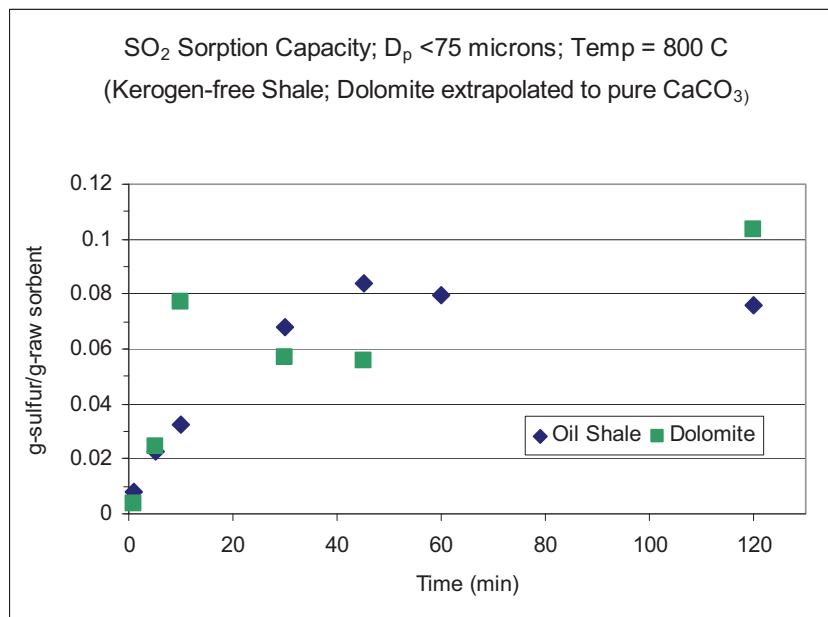


Figure 10. Comparison of oil shale particle sorption capacity to dolomite limestone.

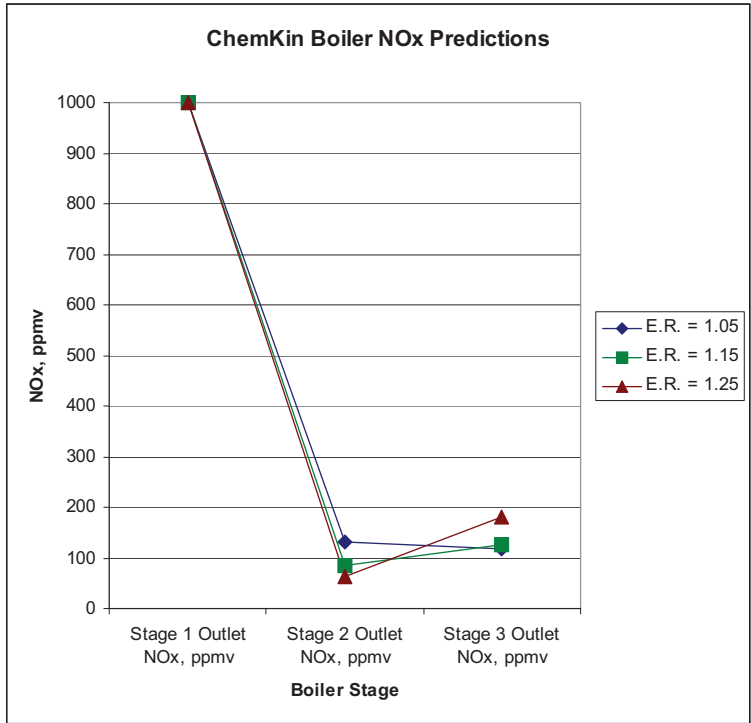


Figure 11. Kinetic prediction of NOx reduction by oil shale volatiles for a two-stage combustor.

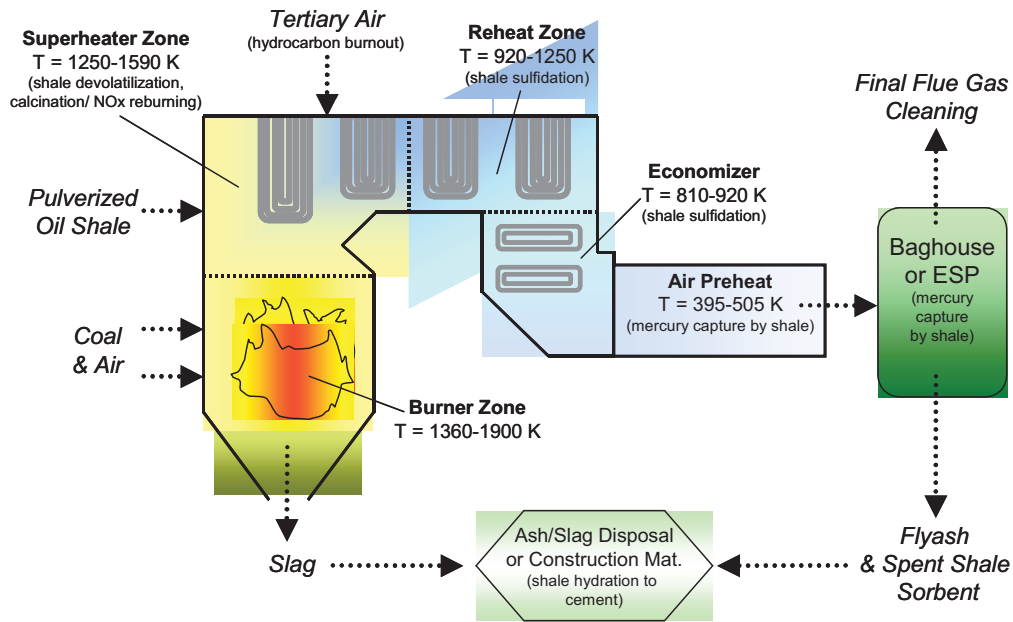


Figure 12. Injection of unreacted, pulverized oil shale into a pulverized coal combustor.